Int. J. Electrochem. Sci., 16**(2021)** Article Number: 211120, doi: 10.20964/2021.11.26

International Journal of ELECTROCHEMICAL SCIENCE
www.electrochemsci.org

Short Communication

Effect of Soil Density and Electrode Material on the Electrokinetic Removal of Pb(II) from Contaminated Silt Soil

Gang Li[1], *Chongkun Chen*[1], *Jia Liu*[2,*], *Yao Zhang*[1], *Shuai Li*[3]

[1] Shaanxi Key Laboratory of Safety and Durability of Concrete Structures, Xijing University, Xi’an, Shaanxi 710123, China;
[2] School of Geological Engineering and Geomatics, Chang’an University, Xi’an, Shaanxi 710054, China;
[3] State Key Laboratory of Coastal and Offshore Engineering, Dalian University of Technology, Dalian, Liaoning 116024, China.
[*]E-mail: 15929935077@163.com

Received: 19 July 2021/ *Accepted:* 3 September 2021 / *Published:* 10 October 2021

With the increase in industrial Pb-containing products, Pb pollution is gradually accumulating in the soil, leading to the degradation of soil quality and damage to human health. To find an efficient and environmental method for the remediation of Pb-contaminated silt soil, electrokinetic remediation (ER) was carried out with different soil densities and electrode materials, and the variation laws of the current (I), potential (U), pH, removal efficiency (R), and energy consumption (E) during the ER process were investigated. The results showed that as the ER time (t) increased, I showed a trend of increasing-decreasing-increasing, while U showed a trend of decreasing-increasing-decreasing. Soil density had a great effect on the soil pH, while the electrode material had a great impact on the catholyte pH. Both Pb(II) R and E decreased with increasing soil density. The maximum Pb(II) R reached 98.13% with a unit E of 1.34 W·h/mg. The Pb(II) R obtained with different electrode materials followed the order of ruthenium-iridium coated titanium mesh>rhodium-iridium coated titanium mesh>ruthenium-iridium coated titanium plate, indicating that the electrode of ruthenium-iridium coated titanium mesh had the best removal effect in the ER of the Pb(II)-contaminated silt soil. The research results can provide a reference for ER projects in Pb(II)-contaminated silt soil areas.

Keywords: Electrokinetic remediation; silt soil; density; electrode; removal efficiency

1. INTRODUCTION

As a toxic heavy metal, Pb can be deposited in the soil and combine with ions to form insoluble substances when industrial Pb-containing products (batteries, dyes, ceramics, warheads, cosmetics, etc.) are abandoned. Consequently, the Pb content in the soil can significantly exceed the background value, and because soil self-remediation is difficult, this pollution eventually leads to soil degradation, ecological destruction, and environmental deterioration [1-3]. Pb pollution has the characteristics of concealment, long-term irreversibility, and bioaccumulation. Therefore, finding an efficient, environmentally friendly, and economical heavy metal pollution remediation technology has become a critical problem to be solved. Electrokinetic remediation (ER) is a soil remediation technology that emerged in the 1980s and is mainly based on electrochemical principles. When electrodes are implanted in a soil solid/liquid system, pollutants can migrate to the electrodes via electro migration, electro-osmosis, or electrophoresis under an electric field, thereby achieving soil remediation [4]. Many scholars have studied the ER of heavy metal-contaminated soil and have verified the reliability of this method. Yuan et al. [5] conducted ER to remove Cd, Cu, Ni, Pb, and Zn from contaminated black soil and concluded that the removal efficiency (R) of heavy metals was higher than 80% in all the tests performed . Based on ER using sodium alginate and chitosan as agents, Wang et al. [6] found that the R of Cu and Zn reached 95.69% and 95.05%, respectively, whereas Pb was difficult to remove from contaminated soil. Luo et al. [7] revealed that the volume of leachate decreased significantly in pots under the effect of ER, while the leaching risk of Pb and Cu deteriorated. Based on ER tests, Fijalkowska et al. [8] discovered that the Pb adsorbed capacity and immobilization effectiveness depended on the polyacrylamide presence and structure of aluminosilicate. Saberi et al. [9] investigated the removal performance of phenanthrene (PHE), Pb, Zn, and Ni from clayey soils based on ER method, and concluded that the highest R of PHE reached 61% and that the R of heavy metals followed the trend of Zn>Ni>Pb. Camesalle et al [10] noted that when the concentration of citric acid (used as a facilitating agent) increased to 0.5 M, the R of Cd, Co, Cu, Zn, Cr and Pb reached 78.7%, 78.6%, 72.5%, 73.3%, 11.8%, and 9.8%, respectively. Based on in-situ leaching and ER tests, Han et al. [11] pointed out that the combined remediation method saved 23.8% of the EDTA dosage, and the removal effects of Cd, Cu, Pb, and Zn were relatively better. Kim et al. [12] compared the removal effect of heavy metals (Cd, Cu, Pb, Ni, and Zn) from contaminated soils by one-dimensional and two-dimensional ER, and demonstrated that the 2D electrode configuration increased the R of the heavy metal ions compared with a 1D array, whereas the energy consumption (E) was increased to a certain extent. Yang and Xi [13] found that an acidic soil environment facilitated the removal of Pb(II) ions. Therefore, pH has a great impact on the remediation of contaminated soil. The effectiveness of ER can be improved by controlling the pH in the cathode region and by controlling the migration of OH^- to the anode. Cai et al. [14] studied the influence of electrode materials on the ER of Pb(II)-contaminated soil. It was found that when the electric field was 1 V/cm and the remediation time (t) was 48 h, R reached 77% with a graphite electrode but only reached 64% and 54% with a stainless steel electrode and titanium electrode, indicating that the graphite electrode provided more active interfaces for electron transfer. Liu and Zhuang [15] studied the effect of different additives on the removal of Pb from contaminated soil and concluded that adding acetic acid could better promote Pb removal than adding citric acid. The main reason was that citric acid and Pb ions tend to form difficult-to-ionize substances that hinder Pb migration, while ethylenediaminetetracetic acid disodium (EDTA-2Na) can complex with most Pb ions to form complex ions. Li et al. [16] used tartaric acid as an electrolyte and found that the R of Cu^{2+}, Mn^{2+}, Cd^{2+}, Pb^{2+}, and Zn^{2+} were 75.67%, 98.11%, 85.1%, 70.75% and 90.9%, respectively. The results indicated that tartaric acid increased the content of weakly acidextracted heavy metals in the soil and promoted the migration of heavy metals, thereby facilitating ER. Wan et al. [17] found that compared with conventional ER, remediation with intermittent energization and exchange electrode energization increased the total *R* of Pb by 8.65% and 31.05%, respectively, while reducing the *E* by 58.03% and 44.90%. The results indicated that intermittent energization and exchange electrode energization significantly improved the removal of Pb from contaminated soil and reduced the *E* in the meantime. Zhang et al. [18] concluded that when EDTA was used as the cathodic control solution, the EDTA reacted with lead nitrate to form soluble complexes, improving the mobility of Pb ions and thereby the remediation effect. As the concentration of EDTA increased from 0.1 mol/L to 0.2 mol/L, the *R* increased from 44.4% to 61.5%, indicating that the addition of the complexing agent significantly improved the remediation of Pb-contaminated soil. Ren et al. [19] reported that when Fe(III)-activated carbon fiber was used to improve ER, the lower the anolyte pH was, the better the Pb removal. The maximum Pb *R* was 80.53%, 53.1%, and 40.69% at anolyte pH values of 3, 4, and 5, respectively. Fang et al. [20] found that EDTA reacted with the OH^- produced by electrolysis to form EDTA anions. Under an electric field, EDTA anions entered the soil and reacted with Pb carbonate to form soluble complexes. The mobility of Pb was improved, resulting in a maximum *R* of Pb up to 82.1%.

Current research results show that a "focusing effect" is likely to occur during the ER process. Therefore, researchers have been seeking to improve the remediation efficiency by selecting specific energization modes, exchanging electrodes, adding electrolytes and enhancers, and adjusting the pH. However, relatively few studies have been conducted on the effect of soil density and electrode material on ER efficiency. In this study, different soil densities and electrode materials were tested to investigate the effect on the ER of Pb-contaminated silt soil. Additionally, the variation laws of the current (*I*), potential (*U*), pH value, removal efficiency (*R*), and energy consumption (*E*) during the ER process were analyzed. The research results can provide a reference for practical engineering of ER in Pb(II)-contaminated silt soil areas.

2. EXPERIMENTAL

2.1 Materials

Silt soil was collected from a green belt without heavy metal contamination at Dalian University of Technology. After the removal of debris, the soil samples were passed through a 2-mm sieve before being dried for later use. Table 1 lists the basic physical characteristics of the silt soil.

Table 1. Physical parameters of the silt soil

Specific gravity	Liquid limit (%)	Plastic limit (%)	Plasticity index
2.64	24.4	16.5	7.9

2.2 Instrument

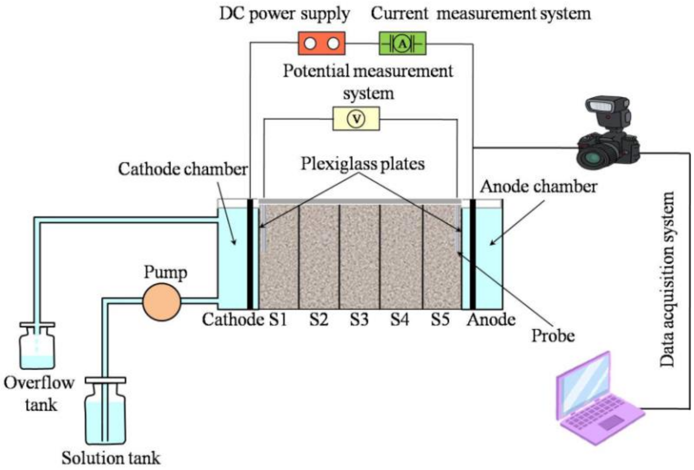

Figure 1. Test equipment

The ER test equipment is shown in Figure 1, and it mainly includes a model box made of plexiglass, a direct current (DC) power supply, an *I* and *U* measurement system, an electrolyte circulation system, an overflow collection system, and a data acquisition system. The model box was 310 mm in length, 90 mm in width, and 120 mm in height. The size of the sample chamber was 100 mm in length, 70 mm in width, and 100 mm in height, the size of the electrode chamber was 70 mm in length, 70 mm in width, and 100 mm in height, and the size of the electrode was 70 mm in length and 100 mm in width. The electrode chamber and the sample chamber were separated by double-layer porous plexiglass plates, and filter paper was placed between the two plexiglass plates to prevent soil particles from entering the electrode chamber. Small holes were situated at the bottom of the electrode chambers on both sides of the soil chamber for the peristaltic pump to pump the circulating electrolyte into the electrode chamber. Overflow holes were opened on both sides of the electrode chamber, and their positions were flush with the soil after loading to ensure that the upper surface of the soil was not covered by electrolyte during the test. The main instruments and equipment used in the test are shown in Table 2.

Table 2. Main instrument and equipment

Instrument	Manufacturer
GPS-2303CDC stabilized power	Good Will Instrument Co., Ltd
DHG-9011A drying oven	Shanghai Jinghong Laboratory Instrument Co., Ltd
CT15RT freezing high speed centrifuges	Shanghai Tianmei Biochemical Instrument and Equipment Engineering Co., Ltd
CP214 analytical balance	OHAUS Instrument (Shanghai) Co., Ltd
FIVEEASY PLUS28 pH meter	Mettler Toledo Instrument (Shanghai) Co., Ltd
AA60000 atomic absorption spectrometer	Shanghai Tianmei Biochemical Instrument and Equipment Engineering Co., Ltd
VC86E digital multimeter	Double King Industrial Holdings Co., Ltd
YZ15 peristaltic pump	Baoding Lead Fluid Technology Co., Ltd

2.3 Method

As shown in Table 3, nine groups of ER tests for Pb(II)-contaminated silt soil were conducted to account for the effect of the soil density and electrode materials. During the test, the water content of the silt soil was controlled at 18%, and the soil density was set at 1.30 g/cm^3, 1.42 g/cm^3, and 1.65 g/cm^3. Furthermore, the *U* was set to 30 V, 0.1 mol/L KNO_3 was used as analyte, and 0.15 mol/L citric acid was used as the electrolyte and circulated in the cathode at a rate of 1 mL/min. The remediation time was set to 4 d, and all the tests were repeated. During the test, the measurement of *I*, *U*, pH, and *C* were performed according to the literature [21].

Table 3. Test scheme

Test No.	Electrode	Soil density (g/cm^3)
T1	Ruthenium-iridium coated titanium mesh	1.30
T2	Rhodium-iridium coated titanium mesh	1.30
T3	Ruthenium-iridium coated titanium plate	1.30
T4	Ruthenium-iridium coated titanium mesh	1.42
T5	Rhodium-iridium coated titanium mesh	1.42
T6	Ruthenium-iridium coated titanium plate	1.42
T7	Ruthenium-iridium coated titanium mesh	1.65
T8	Rhodium-iridium coated titanium mesh	1.65
T9	Ruthenium-iridium coated titanium plate	1.65

To prepare the Pb(II) contaminated soil with a concentration of 1000 mg/kg, firstly, 2000 g of dried silt soil, and a sufficient amount of distilled water were measured, and 3.1969 g of $Pb(NO_3)_2$ was dissolved in a beaker. Secondly, the $Pb(NO_3)_2$ solution was added to the dry soil, and the beaker and glass rod were washed with distilled water two to three times. Distilled water was added to the soil until the soil was in a flow-plastic state, and the soil sample was stirred with a stirrer for 1 h to evenly distribute the Pb(II) in the soil. Subsequently, the soil was dried and crushed, and passed through a 2-mm sieve. The water content of contaminated soil was controlled at 18% by spraying water, and follow by put into ziplock bag to equilibration for 48 h. Finally, in order to prepare soil density of 1.30 g/cm^3, 1.42 g/cm^3 and 1.65 g/cm^3, the mass of contaminated soil was set at 910 g, 994 g and 1155 g due to the sample volume was 700 cm^3. After the sample was loaded layer by layer in the sample chamber, the electrolyte was injected into the electrode chamber, followed by equilibration for 48 h. After the ER tests, four thin metal sheets were inserted into the soil sample chamber at an interval of 2 cm, and the soil was divided into five equal parts. A spoon was used to dig out the soil, the areas from the cathode to the anode were labeled as S1-S5 sequentially, and the soil was dried for testing.

The Pb(II) R and E were calculated as follows:

$$R=\frac{\left(m_0-m_e\right)}{m_0}\times 100\% \tag{1}$$

where R is the removal efficiency, %; m_0 is the initial total mass of pollutants, mg; and m_e is the total mass of remaining pollutants, mg.

$$E_c=\frac{1}{M_c}\int UIdt \tag{2}$$

where E_c is the electric consumption for removing a unit mass of pollutants, W·h/mg; M_c is the total amount of pollutants removed, $M_c=m_0-m_e$, mg; U is the potential, V; I is the current, A; and t is the treatment time, h.

3. RESULTS AND DISCUSSION

3.1 Effect of current

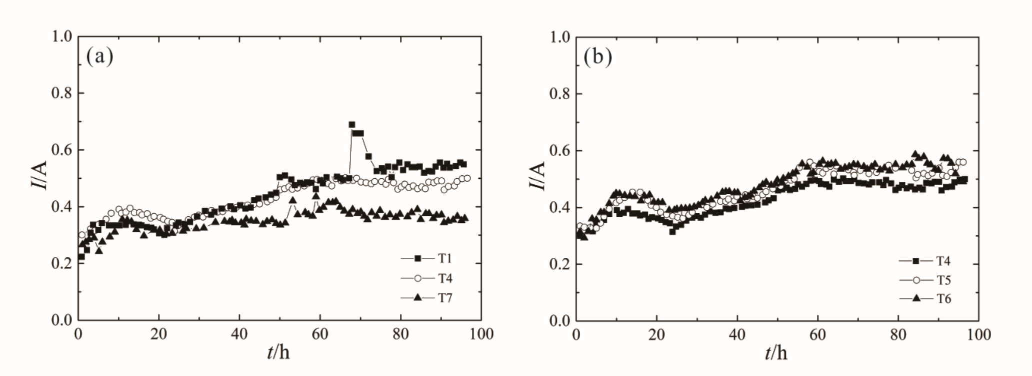

Figure 2. Dependence of current on remediation time during electrokinetic remediation with 30 V potential, 1000 mg/kg initial concentration, and 0.15 mol/L citric acid as the catholyte (a) influence of density, (b) influence of electrode material

Figure 2 shows the curves of I versus t during the ER process. As t increased, the I showed an overall trend of increasing-decreasing-increasing. The I achieved the peak at 15 h and reached a stable state at 80 h. When the soil density was 1.30 g/cm^3 (T1), the stabilized I was relatively large, and when the soil density was 1.65 g/cm^3 (T7), the stabilized I was relatively small. Therefore, soil density had a great influence on I. As the soil density increased, the stabilized I also decreased. Figure 2(b) shows that the variation laws of I with different electrode materials were basically consistent. The magnitude of I followed the order of ruthenium-iridium coated titanium plate (T6)>rhodium-iridium coated titanium mesh (T5)>ruthenium-iridium coated titanium mesh (T4). E was high when a ruthenium-iridium coated titanium plate was used as the electrode, and the E was low when a ruthenium-iridium coated titanium mesh was used as the electrode. Generally, the concentration of mobile ions in the soil during the ER process directly affects the magnitude of *I*. The higher the *U* is, the higher the concentration of free ions is, and the faster the *I* changes [22].

3.2 Effect of potential

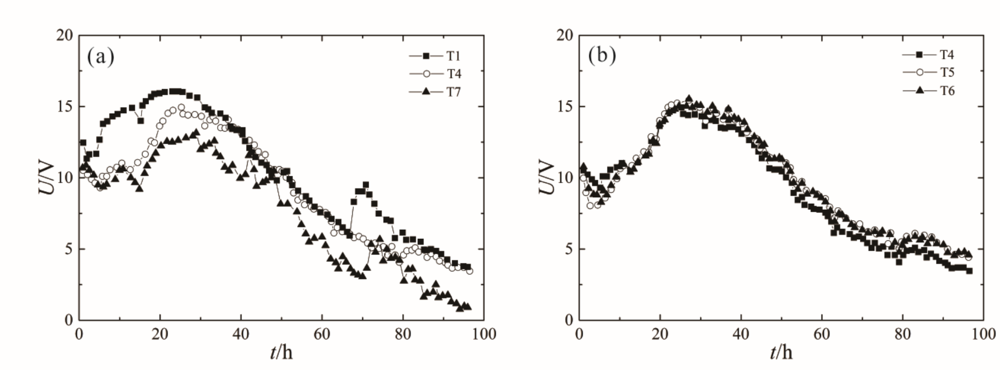

Figure 3. Dependence of potential on remediation time during electrokinetic remediation with 30 V potential, 1000 mg/kg initial concentration, and 0.15 mol/L citric acid as the catholyte (a) influence of density, (b) influence of electrode material

Figure 3 shows the curves of *U* versus *t* during the ER process. As *t* increased, the *U* showed an overall trend of decreasing-increasing-decreasing. The *U* reached the maximum at 30 h and then began to gradually decrease. The results obtained using different soil densities were compared. Similar to *I*, the *U* was low when the soil density was 1.65 g/cm^3 (T7) and was high when the soil density was 1.30 g/cm^3 (T1), indicating that the *U* gradually decreased as the soil density increased. Figure 3(b) shows that the *U* under different electrode materials exhibited the same trend and that the difference between tests was small. When ruthenium-iridium coated titanium mesh (T4) was used as the electrode, the *U* was relatively small; when rhodium-iridium coated titanium mesh (T5) or ruthenium-iridium coated titanium plate (T6) was used as the electrode, the *U* was relatively large. Generally, *U* is an important factor that affects the ER efficiency, as reflected in three aspects: (1) the greater the *U* gradient is, the more violent the reaction is, and the faster the pH changes, so H$^+$ generated by a pH change can better facilitate the migration of metal ions; (2) the greater the *U* gradient is, the stronger the electric field force on the metal ions is, so the higher the *R* is; and (3) the *U* gradient can directly affect electro-osmotic flow, creating an important force that drives the migration of ions in the interstitial water of the soil [23].

3.3 Effect of pH

Figure 4 shows the curves of electrolyte pH versus *t* during the ER process. To control the catholyte pH and facilitate Pb(II) removal, a peristaltic pump was used to continuously pump 0.15 mol/L citric acid solution to the cathode to ensure that the cathode pH was acidic. The anolyte pH was in the range of 0~2, while the catholyte pH was in the range of 2~6. Acidic conditions were beneficial to the ER process. In addition, as the soil density increased, the anolyte pH and catholyte pH changed little, indicating that soil density had a small effect on the electrolyte pH. Figure 4(b) shows that when different electrode materials were used, the difference in anolyte pH was small, while the difference in catholyte pH was relatively large. When ruthenium-iridium coated titanium mesh was used as the electrode, the electrolyte pH was significantly higher than that of the rhodium-iridium coated titanium mesh and ruthenium-iridium coated titanium plate.

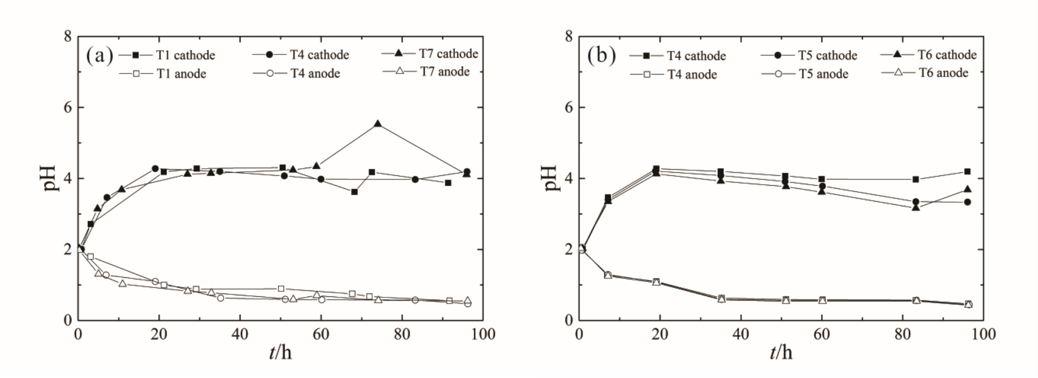

Figure 4. Dependence of electrolyte pH on remediation time during electrokinetic remediation with 30 V potential, 1000 mg/kg initial concentration, and 0.15 mol/L citric acid as the catholyte (a) influence of density, (b) influence of electrode material

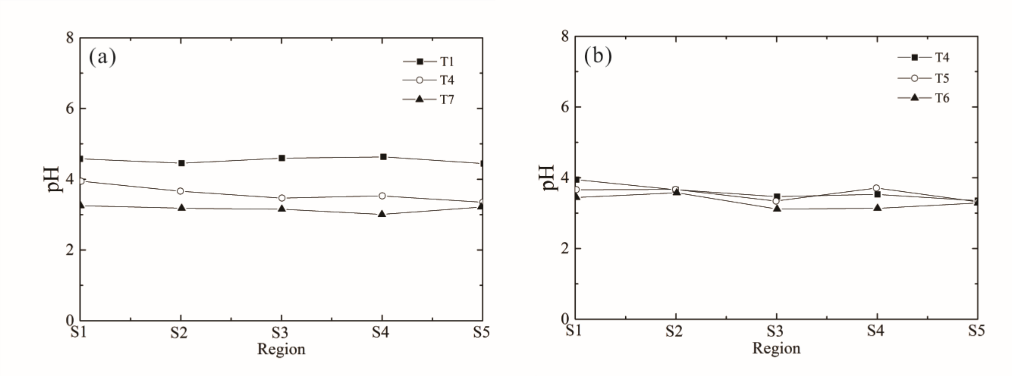

Figure 5. Dependence of soil pH on region after electrokinetic remediation with 30 V potential, 1000 mg/kg initial concentration, and 0.15 mol/L citric acid as the catholyte (a) influence of density, (b) influence of electrode material

During the ER process, the *R* can be effectively improved by controlling the pH at both electrodes. At the anode, H^+ is continuously produced during the reaction. To avoid soil acidification and anode corrosion, the lower limit of pH needs to be controlled. At the cathode, OH^- produced by electrolysis changes the form of heavy metals, resulting in poor pollutant removal [24]. Figure 5 shows the curve of soil pH versus region after ER. S1 is the area close to the cathode side, and S5 is the area close to the anode side. The soil pH was between 3 and 5, and the soil pH near the cathode was slightly higher than that near the anode. The pH distributions under different soil densities are compared in Figure 5(a). The soil pH was high when the soil density was 1.30 g/cm^3 and was low when the soil density was 1.65 g/cm^3, indicating that the soil pH decreased as the soil density increased. Figure 5(b) shows that the soil pH was similar when different electrode materials were used. The soil pH obtained using the ruthenium-iridium coated titanium plate as the electrode was significantly lower than those obtained using the ruthenium-iridium coated titanium mesh and rhodium-iridium coated titanium mesh.

3.4 Effect of Pb(II) concentration

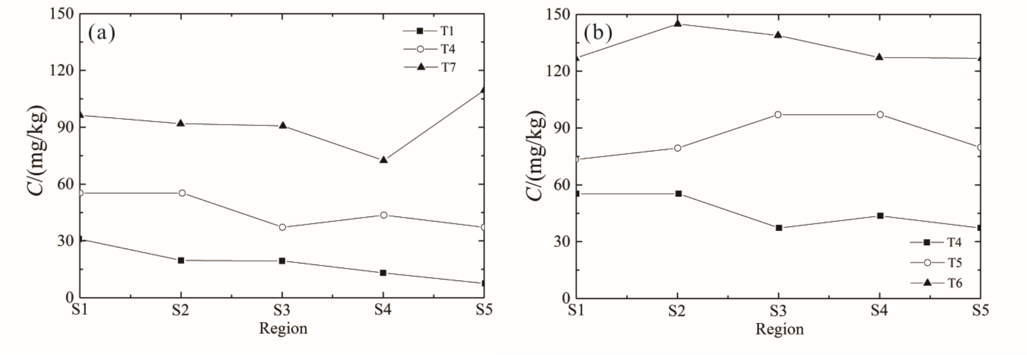

Figure 6. Dependence of Pb(II) concentration on region after electrokinetic remediation with 30 V potential, 1000 mg/kg initial concentration, and 0.15 mol/L citric acid as the catholyte (a) influence of density, (b) influence of electrode material

Figure 6 shows the curves of Pb(II) concentration (*C*) versus region after ER. The Pb(II) *C* in the cathode region was slightly higher than that in the anode region, indicating that Pb(II) had migrated from the anode to the cathode under the electric field. The *C* of Pb(II) was higher in certain regions, indicating that these regions were rich in Pb(II). The Pb(II) *C* in the soil was low when the soil density was 1.30 g/cm^3 and was high when the soil density was 1.65 g/cm^3. This result indicated that as the soil density increased, the *C* of Pb(II) in the soil gradually increased, and the corresponding Pb(II) *R* gradually decreased. Figure 6(b) shows that the Pb(II) *C* in the soil was significantly different when different electrode materials were used. Pb(II) *C* followed the order ruthenium-iridium coated titanium plate>rhodium-iridium coated titanium mesh>ruthenium-iridium coated titanium mesh. Thus, when the ruthenium-iridium coated titanium mesh was used as the electrode, the Pb(II) *C* in the soil was the lowest, and the Pb(II) *R* was the highest.

3.5 Removal efficiency and energy consumption

Table 4 summarizes the Pb(II) *R* and *E* of different tests after ER. The Pb(II) *R* of T1 reached 98.13%, and the unit *E* was only 1.34 W·h/mg, while the Pb(II) *R* of T9 was only 84.56%, and the unit *E* was 1.39 W·h/mg. The high Pb(II) removal was attributed to the addition of citric acid. Citric acid has a strong desorption ability, is easy to degrade, and can form soluble citrate with heavy metals, thereby improving the ER efficiency [10, 25]. As the soil density increased, both the Pb(II) *R* and *E* gradually decreased. Among the different electrode materials, the ruthenium-iridium coated titanium mesh electrode exhibited the highest Pb(II) *R* and the lowest *E*. Therefore, it was concluded that for the

ER of Pb(II)-contaminated low-density silt soil, good remediation can be achieved by using ruthenium-iridium coated titanium mesh as the electrode. Table 5 lists a comparison of Pb(II) removal by ER method. Although the adopted electrode material, potential gradient and initial concentration were different, the Pb(II) *R* varied from 30.00% to 98.13%, especially the highest *R* attained in this study.

Table 4. Pb(II) removal efficiency and energy consumption after electrokinetic remediation

Test No.	Removal efficiency (%)	Energy consumption (kW·h)	E_c (W·h/mg)
T1	98.13	1.27203	1.34
T2	94.65	1.38249	1.51
T3	89.18	1.36203	1.58
T4	95.27	1.22697	1.34
T5	91.17	1.33692	1.52
T6	86.19	1.37851	1.66
T7	90.42	0.99998	1.14
T8	89.55	1.16252	1.34
T9	84.56	1.13204	1.39

In addition, the *E* obtained in this study was higher than that of references [29, 38] and significantly lower than that of reference [37]. Therefore, it can be concluded that for low-density soil, when a ruthenium-iridium coated titanium mesh is used as an electrode, an effective removal effect can be achieved for Pb(II) contaminated soil.

Table 5. Comparison of Pb(II) removal by electrokinetic remediation

Electrode	Potential gradient (V/cm)	Initial concentration (mg/kg)	Removal efficiency (%)	Energy consumption	Reference
Graphite	1.0	853.25	50.08	302.00 kW·h/t	[26]
Platinum	--	450.00	30.00	0.44 kW·h/kg	[27]
Graphite	1.0	63.93	60.00	45.10 kW·h/t	[28]
Graphite	1.0	402.20	64.31	0.01 kW·h	[29]
Graphite	2.0	3668.00	36.00	307.20 kW·h/m^3	[30]
Graphite	1.0	1000.00	69.00	58.00 kW·h/m^3	[31]
Graphite	1.0	145.00	80.53	0.43 kW·h/g	[32]
Graphite	2.0	2194.00	31.50	224.00 kW·h/m^3	[33]
Graphite	1.0	550.00	62.00	27.00 kW·h/m^3	[34]
Graphite	1.0	700.00	82.78	25.55 kW·h/kg	[35]
Titanium	2.0	10594.00	40.40	34.80 kW·h/m^3	[36]
Graphite	1.5	940.83	80.37	3.46 kW·h	[37]
Steel	2.0	1000.00	32.52	0.92 kW·h	[38]
Titanium	3.0	1000.00	98.13	1.27 kW·h	This study

4. CONCLUSIONS

(1) As *t* increased, the *I* showed an overall increasing-decreasing-increasing trend. As the soil density increased, the stabilized *I* decreased. The *I* magnitude under different electrode materials followed the order of ruthenium-iridium coated titanium plate>rhodium-iridium coated titanium mesh>ruthenium-iridium coated titanium mesh.

(2) As *t* increased, the *U* showed an overall decreasing-increasing-decreasing trend. *U* gradually decreased as the soil density increased. *U* was relatively small when a ruthenium-iridium coated titanium mesh was used as the electrode and was relatively large when a rhodium-iridium coated titanium mesh or ruthenium-iridium coated titanium plate was used as the electrode.

(3) Soil density had a small effect on the electrolyte pH but had a large effect on the soil pH. Electrode material had a great impact on the catholyte pH but had a small impact on the soil pH.

(4) With the same electrode material, the Pb(II) *R* decreased with increasing soil density; with the same soil density, the Pb(II) *R* followed the order of ruthenium-iridium coated titanium mesh>rhodium-iridium coated titanium mesh>ruthenium-iridium coated titanium plate.

(5) When a ruthenium-iridium coated titanium mesh was used as the electrode for the ER of Pb(II)-contaminated low-density silt soil, a high Pb(II) *R*, low *E*, and a good remediation effect were achieved.

ACKNOWLEDGEMENTS

This work was supported by the Natural Science Basic Research Program of Shaanxi Province (2021JM-535), and Special Fund for Scientific Research by Xijing University (XJ18T01).

CONFLICT OF INTEREST

On behalf of all authors, the corresponding author states that there is no conflict of interest.

References

1. Y.Z. Zhang, B. Wang, Q. Cheng, X.L. Li and Z.Y. Li, *J. Nanosci. Nanotechnol.*, 20 (2020) 7231.
2. A.O. Fayiga and U. Saha, *Chemosphere*, 160 (2016) 252.
3. A.M. Massadeh, M.Y. EI-Khateeb and S.M. Ibrahim, *Public Health*, 149 (2017) 130.
4. X.S. Song, J. Xie, Y.H. Wang, B. Yang, Z.L. Zhang and S.Y. Wang, *J. Saf. Environ.*, 20 (2020) 1542.
5. L.Z. Yuan, X.J. Xu, H.Y. Li, Q.Y. Wang, N.N. Wang and H.W. Yu, *Electrochim. Acta*, 235 (2017) 604.
6. Y.C. Wang, Z.J. Han, A. Li and C.W. Cui, *Environ. Pollut.*, 283 (2021) 117111.
7. J. Luo, X.L. Xing, S.H. Qi, J. Wu and X.W.S. Gu, *Chemosphere*, 216 (2019) 661.
8. G. Fijalkowska, M. Wisniewska, K. Szewczuk-Karpisz, K. Jedruchniewicz and P. Oleszczuk, *Chemosphere*, 276 (2021) 130088.
9. N. Saberi, M. Aghababaei, M. Ostovar and H. Mehrnahad, *J. Environ. Manage.*, 217 (2018) 897.
10. C. Cameselle, S. Gouveia and A. Cabo, *Appl. Sci.*, 11 (2021) 1799.
11. H. Han, J. Zhai, A.W. Wang, J. Li, C.D. Xu and Y.S. Wan, *Agric. Biotechnol.*, 9 (2020) 73.
12. S.O. Kim, J.Y. Jeong, W.C. Lee, S.T. Yun and H.Y. Jo, *J. Soils Sediments*, 2020. Doi: 10.1007/s11368-020-02803-z.
13. Y. Yang and Y.H. Xi, *Chin. J. Underground Space Eng.*, 7 (2011) 1329.

14. Z.P. Cai, W.X. Wang and W.S. Li, *Environ. Sci. Manage*., 41 (2016) 108.
15. Z.T. Liu and Y.F. Zhuang, *Chin. J. Geotech. Eng*., 42 (2020) 1359.
16. C. Li, W.R. Fan, Z.B. Yue, Z.H. Wan and J. Wang, *Chin. J. Environ. Eng*., 13 (2019) 2675.
17. Y.S. Wan, H. Han, M. Shen, X. Wen and M.X. Wang, *J. Changzhou Univ.* (*Nat. Sci. Ed.*)., 30 (2018) 66.
18. T. Zhang, H. Zou, Y.N. Wang and X.Y. Han, *Chin. J. Environ. Eng*., 7 (2013) 3619.
19. W.T. Ren, F. Zhu, J. Zhang, Y. Luo and T Liu, *Chin. J. Environ. Eng*., 11 (2017) 6184.
20. Y.F. Fang, Y.Y. Zheng, N. Tang and L.K. Cai, *J. Agro-Environ. Sci*., 27 (2008) 612.
21. G. Li, J.L. Zhang, J. Liu, S.S. Yang and S. Li, *Int. J. Electrochem. Sci*., 16 (2021) 210926.
22. Y.S. Wan, M. Shen, Y.Q. Chen, H. Han, X. Wen and M.X. Wang, *Chin. J. Environ. Eng*., 12 (2018) 2075.
23. C. Cameselle, *Electrochim. Acta*, 181 (2015) 31.
24. J. Hou, L. Fan, M.Y. Zhou, X.F. Zhu, J. Guan and G.L. Gao, *Environ. Eng*., 35 (2017) 185.
25. Y. Zheng, Y.J. Yan, L. Yu, H.L. Li, B.Q. Jiao, Y. Shiau and D.W. Li, *Environ. Sci. Pollut. Res*., 27 (2020) 5572.
26. P. Zhang, C.J. Jin, Z.F. Sun, G.H. Huang and Z.L. She, *Water Air Soil Pollut*., 227 (2016) 217.
27. K.B. Pedersen, P.E. Jensen, L.M. Ottosen and J. Barlindhaug, *Eng. Geol*., 238 (2018) 52.
28. Y. Song, M.T. Ammami, A. Benamar, S. Mezazigh and H.Q. Wang, *Environ. Sci. Pollut. Res*., 23 (2016) 10577.
29. Y.S. Ng, B.S. Gupta and M.A. Hashim, *Environ. Sci. Pollut. Res*., 23 (2016) 546.
30. G. Asadollahfardi, M.S. Sarmadi, M. Rezaee, A. Khodadadi-Darban, M. Yazdani and J.M. Paz-Garcia, *J. Environ. Manage*., 279 (2021) 111728.
31. K.N.O. Silva, S.S.M. Paiva, F.L. Souza, D.R. Silva, C.A. Martinez-Huitle and E.V. Santos, *J. Electroanal. Chem*., 816 (2018) 171.
32. Z.C. Zhang, W.T. Ren, J. Zhang and F. Zhu, *Environ. Technol*., 42 (2021) 884.
33. O.A. Ahmed, *J. Environ. Sci. Health., Part A*, 55 (2020) 1.
34. L. Rajic, B. Dalmacija, M. Dalmacija, S. Roncevic, S.U. Perovic, *Electrochim. Acta*, 86 (2012) 36.
35. Y.S. Ng, B.S. Gupta and M.A. Hashim, *Sep. Purif. Technol*., 156 (2015) 403.
36. C. Li, H.J. Hou, J.K. Yang, S. Liang, Y.F. Shi, R.N. Guan, Y. Hu, X. Wu, J.P. Hu and L.L. Wang, *Clean-Soil Air Water*, 47 (2019) 1800337.
37. Y.J. Zhang, G.H. Chu, P. Dong, J. Xiao, Q. Meng, M. Baumgartel, B. Xu and T. Hao, *J. Soils Sediments*, 18 (2018) 1915.
38. D.D. Wen, R.B. Fu, W. Zhang and Y.Y. Gu, *Environ. Sci*., 38 (2017) 1209.